

GT2011-4* %\$&

Analysis of a Concept for a Low Wind Speed Tolerant Axial Wind Turbine

Ali A. Ameri¹

The Ohio State University

Majid Rashidi²

Cleveland State University

ABSTRACT

In this paper, the authors analyze a design for a wind tower intended for areas of low wind speeds. The wind tower consists of a combination of several rooftop size turbines arranged alongside a cylindrical structure that acts as a Wind Deflecting Structure (WDS). The WDS amplifies the effective wind speed thus allowing the turbine rotors to operate under lower ambient wind speeds. Analyses were performed using simple models as well as more sophisticated CFD methods employing Steady and Unsteady Reynolds Averaged Navier-Stokes methodology. The effect of the wind amplification was shown on a commercial small wind turbine power output map. Also, a wind turbine rotor flow was computed as operating alongside the WDS and compared to the computed operation of isolated turbines at equal effective and ambient wind velocities. The computational analyses of this work suggest that the power output of isolated rooftop wind turbines deployed at low to moderate wind speed may be matched by installing wind turbines alongside a cylindrical wind deflecting structure operating at lower wind speeds. Other benefits of the arrangement are also enumerated.

INTRODUCTION

Wind energy is a growing means of energy generation supplying 2% of the U.S. total energy usage. Domestic US total installed wind energy capacity grew by an annual average of 39% in five years ending in 2009 [1]. This has been achieved using utility scale wind turbines. Technologies such as the one shown in Fig. 1 are especially useful for urban deployment as they require less land and can be erected on roof tops or next to existing structures.

One important limitation placed on the deployment of wind

turbines is the low speed of the wind. Another issue with large wind turbines is the complexity of these machines which is mainly due to their sizes. Use of a Wind Deflecting Structure (WDS) in the form of a cylindrical tower has been demonstrated to amplify the effective wind speed thus allowing wind turbines to be deployed in regions where the wind speed is too low for conventional horizontal axis wind turbines. The design shown in Fig. 1, an example of the foregoing, improves the viability of wind turbines for urban areas by reducing their size. The WDS also helps to increase the hours of operation by reducing the cut-in speed thus allowing the turbine to be utilized efficiently during times when conventional wind turbines are not operable. The clusters of smaller wind turbines would likely not require a gearbox transmission system and would be lighter and easier to deploy and maintain.

The concept for wind turbines analyzed in this paper, to allow improved performance under conditions of low wind speeds, is not unique and there have been other attempts each having certain advantages and disadvantages. Reference [2] contains one other example of taking advantage of deflecting structures. The proposed wind tower, analyzed in this paper, similar to what is shown in Fig. 1, consists of an array of several smaller size rotors arranged alongside a cylindrical structure that acts as a WDS.

Use of CFD as a tool to more quickly screen designs and allow testing of new ideas has become commonplace in aerospace industry. CFD was used here to demonstrate the improved operation under low wind speeds of a rotor cluster such as shown in Fig. 1. Analyses were performed using simple models as well as more sophisticated CFD methods employing Unsteady Reynolds Averaged Navier-Stokes methodology. This paper shows, through such analyses, that the present arrangement of wind turbines may enhance the viability of wind turbines for urban areas by improving the performance through the use of the wind turbine clusters and the tower

¹ Research Scientist

² Betty L. Gordon Distinguished Professor

(WDS). This improvement is achieved by:

- Amplification of the speed of incoming wind using the cylinder thus allowing smaller size rotors per unit power generated leading to reduction of the complexity and cost of the machine.
- Allowing the wind turbine cluster to operate while the ambient wind speed is too low to be used for a conventional design thus increasing the hours of operation in the lower end of the wind speed distribution and additional harnessed energy.

In this paper, first, an analysis of the impact of the relative sizes of the WDS and the turbine rotors is presented. This was done using CFD. The diameter ratio of the WDS to the rotor was translated to a speed amplification factor and through the use of a typical performance map of a small turbine this speed amplification was converted to an increase in power output. In the second part of the paper, a CFD analysis of steady and unsteady rotor flow was carried out showing that the combination of the rotor and WDS indeed has merit and may be a viable option when wind speeds are low. In the following, the computations are described and supporting results are presented.

RESULTS

Effect of Relative Sizes of Rotor and the Wind Deflecting Structure

The ratio of the diameter of the cylindrical WDS to that of the rotor is an important variable in this study. The amplification provided by the WDS varies with this ratio. The larger the ratio, the higher the average speed of the flow at the rotor's face. This relationship was shown through a CFD analysis of the flow around a cylinder and computation of the area-averaged incoming velocity in the region where the rotor would be placed. The resulting information was used to investigate the effect of the size of Wind Deflecting Structures on the wind speed-power curve.

Figure 2 shows a cut of the computational domain and the grid constructed for the computation of the flow around the cylinder. Fig. 3 shows a cross section of the computational domain including the WDS. The area over which the velocity was averaged is marked using a "net" in that figure. Computations were performed using various WDS diameters while the area of the rotor was held fixed.

Figure 4 shows the amplification of the flow speed as a function of the ratio of diameters. The amplification is the ratio of the average speed of flow in the area where the rotor would be deployed to free stream velocity. To check the CFD, computations were made using Potential Theory [3] which agree with the CFD results. One additional CFD computation using unsteady analysis was carried out. The results, as expected, show that increasing the relative diameter of the WDS indeed increases the average speed of the air around the structure. The two data points for the unsteady computations in Fig. 4 come from averages obtained on the two opposite sides of the cylinder giving two slightly different results because of



Figure 1: Model of the wind turbine cluster erected in Cleveland, Ohio

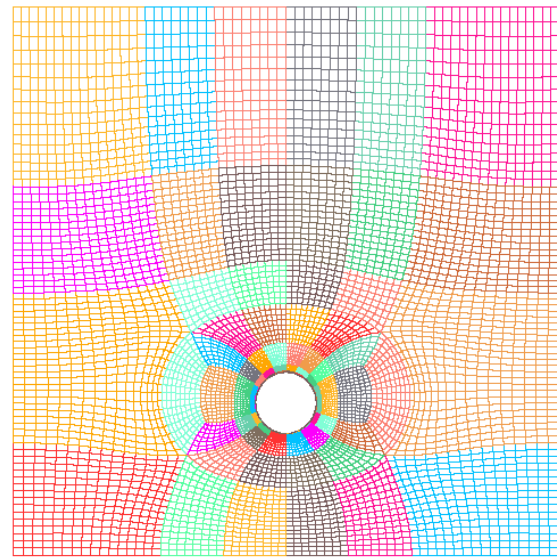


Figure 2: Section of grid for flow around the WDS

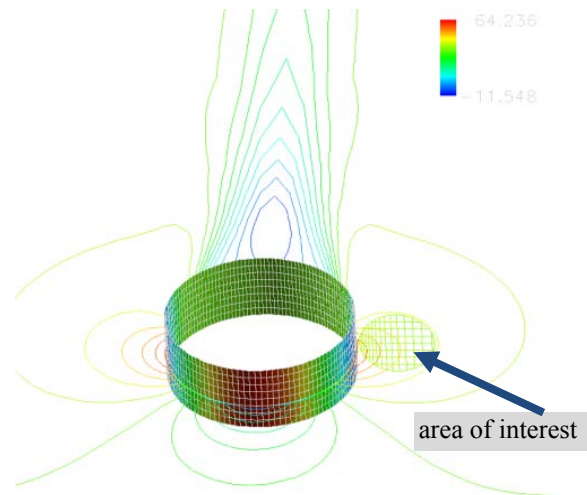


Figure 3: velocity contours around the WDS.

asymmetry of unsteady flow. The data presented in this figure can be used to determine the size requirements based on the distribution of the wind speeds. Figure 4 shows that a diameter ratio of four, results in an increase of wind speed at the rotor by about 60%. As the power output of wind turbine is proportional to the cube of the incoming wind velocity, a 60% increase in wind speed could more than quadruple the power output of the turbine.

Figure 5 shows a typical power curve for a small 6 feet stand alone wind turbine designated as “base line”. The figure shows how the power curve shifts to the left when this turbine is placed next to towers of increasing diameters. It is interesting to note that while the isolated (baseline) rotor achieves best power performance in the ambient wind speed range of 30 to 46 mph (13 to 20 m/s), using a WDS with a radius ratio of about 2.5, the best performance for the particular turbine is obtained for the ambient wind speed range of 18 to 30 mph (or 8 to 13 m/s). Additionally, the WDS effectively reduces the cut-in speed by the inverse of the amplification factor. The amount of energy harnessed over a year can be computed using a Weibull probability distribution for the wind speed [4]. As the distribution of the wind speed is skewed to the lower speed range, the amount of energy captured when using WDS can be multiple times that of the isolated rotor. The effect of the WDS can be determined from this type of analysis. Using the power curve for a small wind turbine, Fig. 5 shows that while at 15 mph wind speed the base line case produces 300 Watts of power, with a 15 ft tower (diameter ratio of 2.5) this level may be increased to 1100 Watts.

Analysis of the Effect of WDS on the Axial Wind Turbine

Two numerical analyses were performed. One, using an isolated rotor and one with a rotor situated alongside a WDS, similar to Fig. 1. They were done using ANSYS-CFX® CFD package. However, initially a test was made to establish the accuracy of the model used.

Test Case

The test case consisted of the NREL Phase VI turbine[5]. This turbine was designed for an NREL research program and tested in the NASA Ames’ 80ft x 120ft wind tunnel. The blades were made with S809 profiles and the distribution of the profile stacking is given in [5]. There are data for pressure distribution on the blade available for example in [6] and elsewhere. Here, this blade profile and radial chord and twist angle distribution were used for all of the CFD runs and the wind turbines were sized to be the same 5 m radius as in [5]. A five bladed arrangement of the blades were used and that same 5 bladed arrangement in a shrouded form was used to test the effect of WDS.

Grid

Figure 6 shows the surface grid and the whole computational domain within which the blades fit. The grid was made as a two zoned/ multiblock structured grid. A disk was formed around the rotor and the grid inside and outside the disk was generated using GridPro®. The size of the domain used for grid generation is shown in Fig. 6. The blade radius is approximately 5m and the domain extent, within the disk zone,

upstream and downstream of the blades is approximately 1.5m. The radius of the disk zone was 6 meters. In order to extend the computational domain beyond the disk zone, another grid was generated and added. The extension of the domain is required to allow specifications of boundary conditions valid for the simulations. This large cylindrical zone has a diameter of 60 meters (6 x rotor diameter). The inlet boundary was place 20 meters (2 x rotor diameter) upstream of the rotor and the exit boundary was placed at 60 meters (6 x rotor diameter) downstream of the rotor. The boundary between the disk and the outer domain is not full face matching and in the process of the flow solution, the flow is interpolated at the boundary between the two zones. One other detail about the inner and the outer grids is that the entire hub of the rotor is not gridded. A cylinder with a small radius passes through the machine, centered along the axis of the machine and this cylinder is modeled as a slip surface in front and beyond the hub. The disk

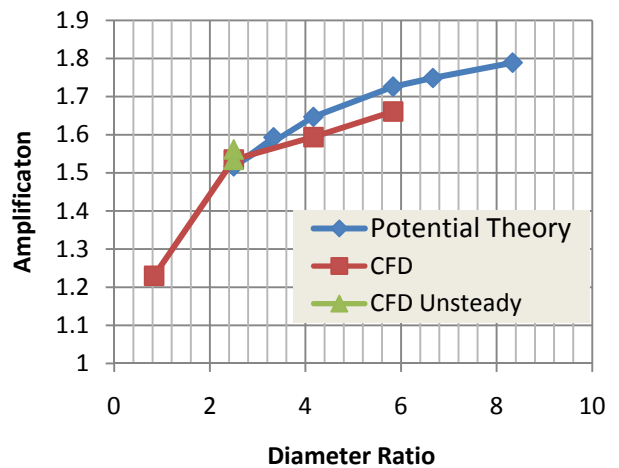


Figure 4: Average amplification of the air velocity for a variety of WDS diameters. The rotor diameter is 6ft.

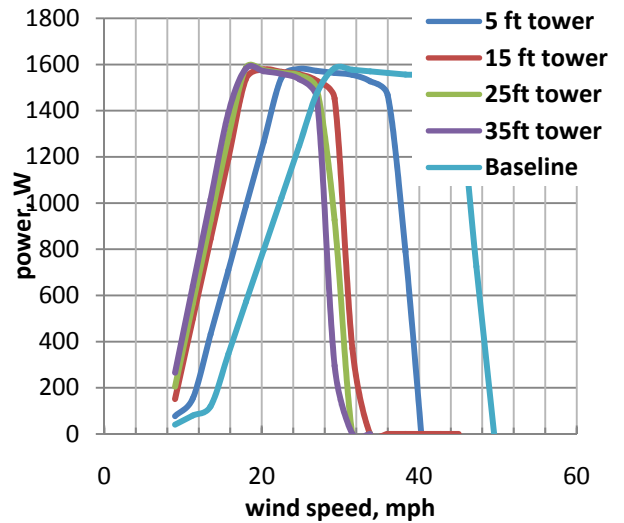


Figure 5: Power curve of a 6 ft diameter turbine rotor as placed in the potential field of towers (WDS) of various sizes.

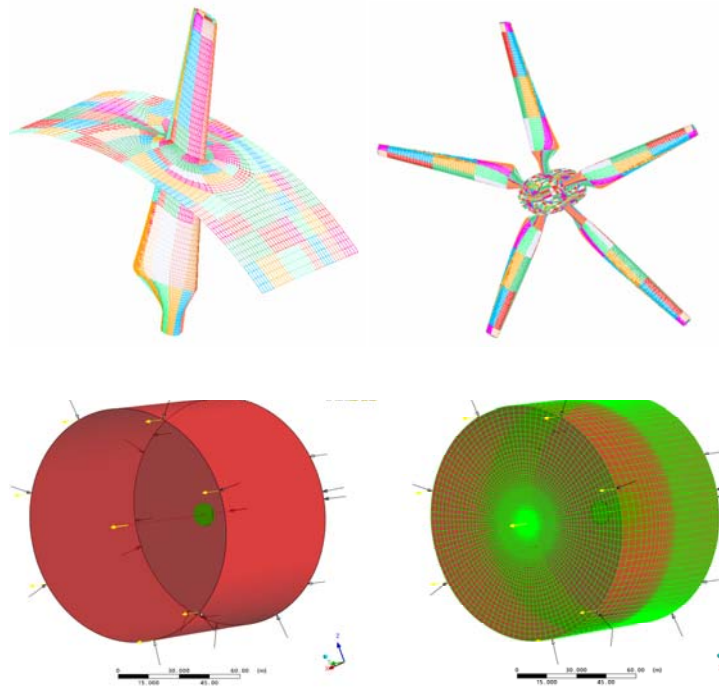


Figure 6: Blade shape and grid for the individual blade and a five-bladed arrangement (above) and placement of the blade domain (Disk) inside the larger domain with structured grid.

and the outer zones designed in this manner make placing the disk in other arrangements possible. For example, the case with the WDS (to be discussed later) may be set up with more ease as only the outer zone grid is required to be modified.

Conditions

The turbine of the NREL experiment consists of three blades rotating at 72 RPM and various wind velocities. For the purposes of this work, a five-bladed arrangement was used, yet the same rotational speed and the lowest wind speed of 7m/sec were employed. The grid for the 5-bladed disk consists of 1.4 million and the outer domain consists of 0.6 million cells totaling about two million cells.

The Numerical Method

The CFX[®] code with the following boundary conditions was

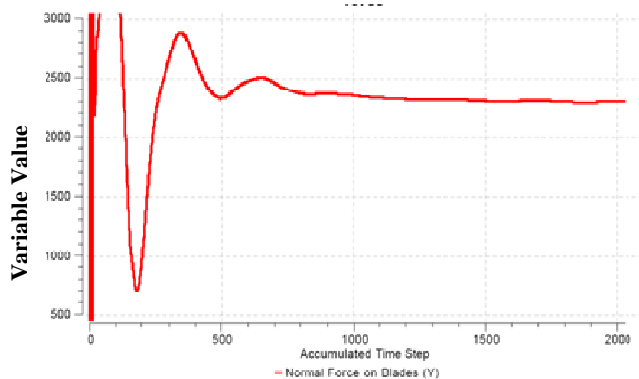


Figure 7: Convergence of the normal force on the blades

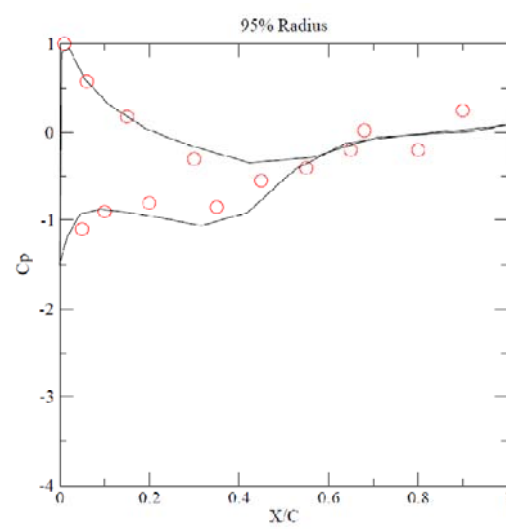
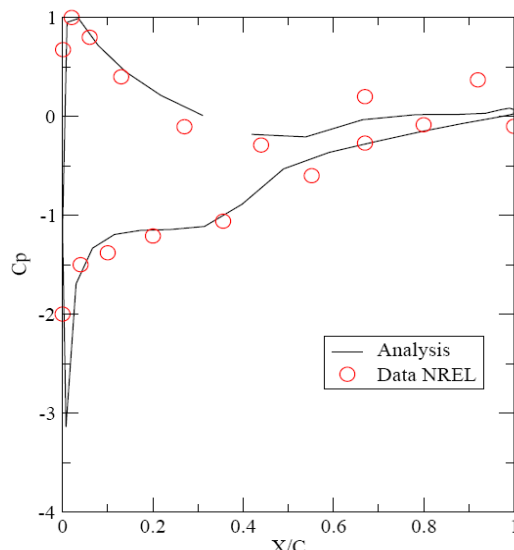
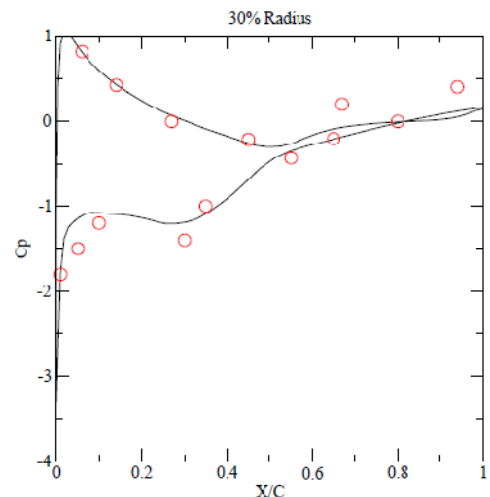


Figure 8: Pressure coefficient at 63% blade height and wind speed of 7m/s at 30, 65 and 95% radius of blade.

used.

- 1- At the inlet boundary constant speed uniform flow was used.
 - 2- A free stream of the same velocity as the inlet was specified around the outer cylinder.
 - 3- At the far exit, constant pressure boundary was used.
- Also, a General Grid Interface condition was used at the interface of the disk and the outer zone.

For the turbulence model, a $K-\omega$ turbulence model which is a 2-equation model [7] was used. The turbulence model applies a wall function if the value of y^+ (dimensionless wall distance) of the first grid point away from the wall is large. Spacing to the walls was such that the average value of y^+ was about a value of two. The highest y^+ value on the blade was four. This occurred in the very tip and very near tip region of the blade. Various criteria were used to monitor convergence of the flow. These included a mass balance, residuals for the momenta and the torque and normal force on the blades. The normal force convergence, as shown in Fig. 7. Pressure distribution at 30%, 63% and 95% blade radial location is shown in Fig. 8. The agreement is good except for near the trailing edge on the suction side due to early separation. For Fig. 8, The variable C_p is defined as:

$$C_p = -(P - P_\infty) / (1/2 * \rho * U_\infty^2)$$

Where U_∞ is defined in terms of the relative incoming velocity. Here ρ is the density and P is the blade surface pressure and P_∞ is the free stream pressure (1 atm.)

Having shown the reasonable agreement with the pressure data and thus the validity of the computational method we proceed to the evaluation of the shrouded turbine.

Evaluation of the Turbine

This part of the work involves the evaluation of the turbine with the WDS. As such a model of a shrouded, five bladed

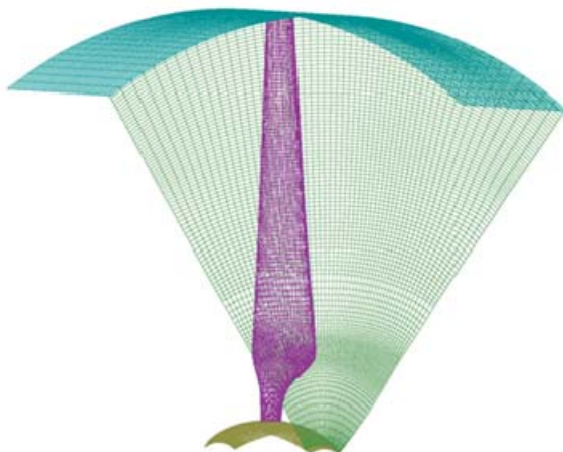


Figure 9: Section of the domain for the shrouded blade

rotor was constructed. A ring of blades formed a disk zone which when embedded in a zone made for the WDS formed the model for the turbine with the WDS and when placed in the large radius domain for the free stream (as in Fig. 6) formed the model for the isolated turbine. The two models were used for investigation of the effect of the WDS.

Three cases were run:

Case 1- Isolated shrouded ring of five blades at 7m/sec free stream velocity

Case 2- Isolated shrouded ring of five blades at 4.6 free stream velocity

Case 3- Shrouded Ring of five blades and WDS at 4.6 m/sec.

Shrouded grid

For the isolated rotor the blade was truncated at the tip to fit a shroud. The resulting grid is shown in Fig. 9 which shows a 72 degree section of the rotor. The 72 degree sections when repeated in a ring form the five-bladed disk. The total number of cells for the isolated rotor and free stream zone grid was 1.7million. For the case which included the Wind Deflection Structure, the general extent of the domain used for simulation is shown in Fig. 10. The WDS is shown in red while the rotors are shown in blue. The sketch is not to scale and is provided to allow a better appreciation for the design of the flow domain. The extent of the grid to where a free-stream boundary condition is to be specified is four times the diameter of the WDS. An overall view of the grid is also shown in Fig. 11 where a close-up of the location of the disk is also provided. The total number of cells for this grid was also approximately 1.7 million. The rotor domain is in contact with the outer domain through zone interfaces. The shroud of the rotor as with the rest of the rotor rotates at the specified speed of rotation having a no-slip condition both on the inner and outer side of the shroud. The close-up view in Fig. 11 also shows the ends of the blade hub. This addition was required because the flow does not approach the rotor parallel to the axis of the rotor due to the presence of the WDS. In the first part of this work, we had a hollow zone consisting of a long, small diameter cylinder through the center of the rotor extending all the way through the rotor. The boundary condition on this cylinder was specified using a slip condition. The assumption was reasonable and the grid generation was, as a result, easier to perform. Here we do not have a hollow region and the whole domain is fully gridded.

Computation Results for the Shrouded Rotor

Case 1- Performance of isolated Rotor at Wind Speed of 7m/sec

The rotor used in the combined rotor and WDS was a shrouded rotor. An isolated shrouded rotor is used to benchmark the turbine and to allow comparison of steady and unsteady models.

The rotor used in the combined rotor and WDS was a shrouded rotor. An isolated shrouded rotor is used to benchmark the turbine and to allow comparison of steady and unsteady models. Here we will show the results of the simulation of the shrouded rotor in steady mode for a wind velocity of 7m/sec and a rotation rate of 72 RPM. The grid arrangement and the boundary conditions are as were used for the earlier simulations of the rotor with unshrouded blades. The domain is large and the radius of the full domain is six diameters of the rotor (as shown in Fig. 6) It also extends six diameters upstream and downstream. The only other condition is that the shroud is a no-slip surface and flux through the shroud is zero.

Figure 12 shows the pressure side and the suction side pressure distribution and the pressure on the shroud. However, the main objective of the CFD computation is to compute the torque on the blade. The torque was computed and the convergence of that quantity is shown in Fig. 13.

There are two lines. One shows the torque due to the normal forces on the blade and the green line is due to tangential forces. The two values are added and the graph suggests a total torque of 600 N-m. This value serves as the goal for the WDS case run at a lower free stream velocity, which is presented next.

Case2- Performance of Isolated Rotor at 4.6m/sec

Assuming an amplification rate of 1.5 for the deployed WDS (based on the diameter ratio and Fig. 4) a free stream velocity of 4.6 m/sec amplifies to the value of 7 m/sec used in the last example. We next ran the isolated wind turbine rotor (without the WDS) at the same rate of rotation of 72 RPM at the lower 4.6 m/sec. We were not able to obtain a stable solution for the torque and a converged solution was not possible.

Case3- Unsteady Analysis of the Rotor including the WDS

Earlier we studied the effect of the WDS using simple models. Here we employ a more sophisticated approach namely, the effect of WDS is evaluated using a CFD model that accounts for the interaction of the wind, WDS and the rotor. A case was set up for this situation and the flow was computed for a “low” wind velocity of 4.6 m/sec or a factor of 1.5 compared to the benchmark case of 7m/sec. Figure 14 shows the contours of air speed in the field. The increase in air speed around the WDS is apparent and shows how the turbine is operating at a higher speed while the upstream wind speed is low. The torque was computed for this flow. The torque was unsteady but the solution was steady in the mean. The solution required nearly 9000 time steps to converge. The unsteady solution was run at steps of 1.2 degrees and 10 iterations per step were required for convergence. The value of torque is the sum of the two components of the torque computed from the tangential and normal components of the force exerted on the blades. The value is 470 N-m for all the blades. This is 78% of the benchmark case at 7m/sec. The amplification factor used appears to be somewhat optimistic.

A stable solution was not obtainable without the WDS. With the WDS we were able to obtain useful torque although the full

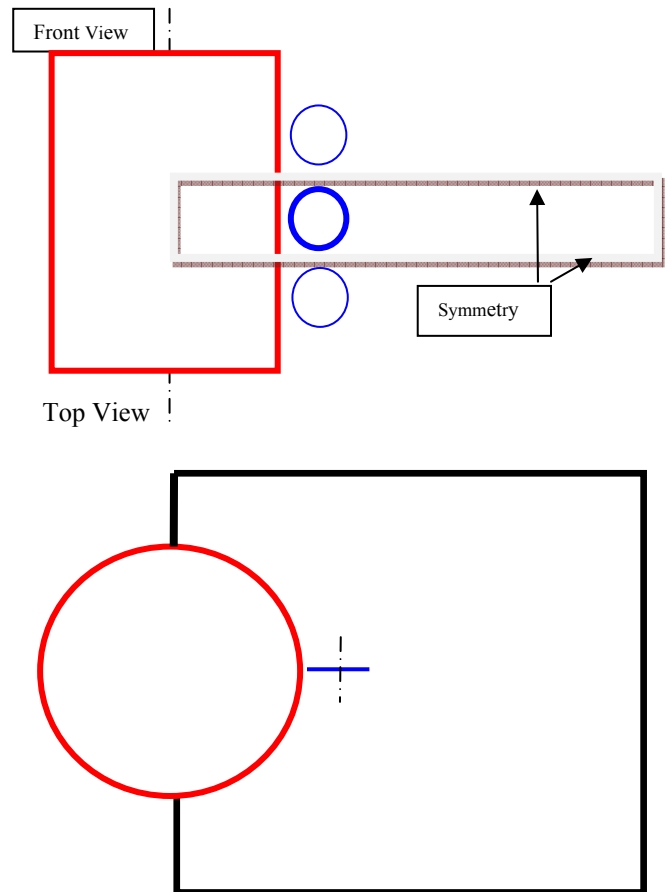


Figure 10: Views of the domain holding the disk and the WDS.

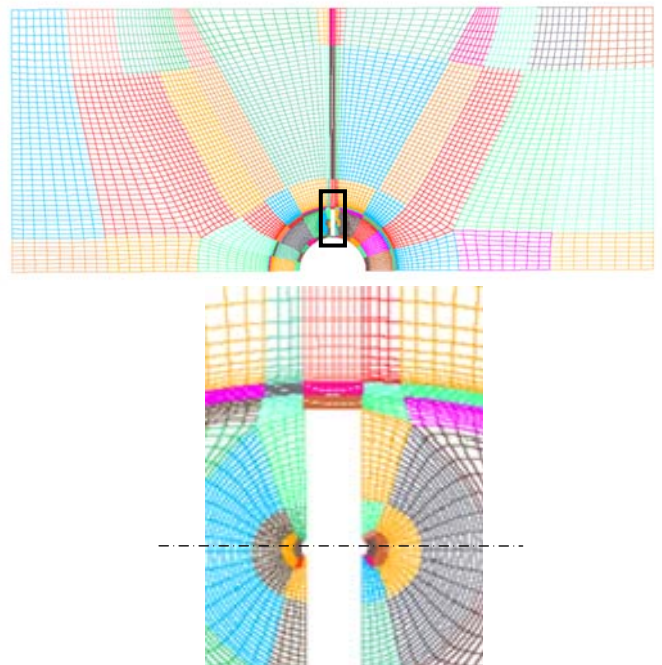


Figure 11: Cut view of the grid for the overall assembly of the rotor and WDS and close-up view of the “hole” in which the disk is placed. Note the extension to the hub of the rotor.

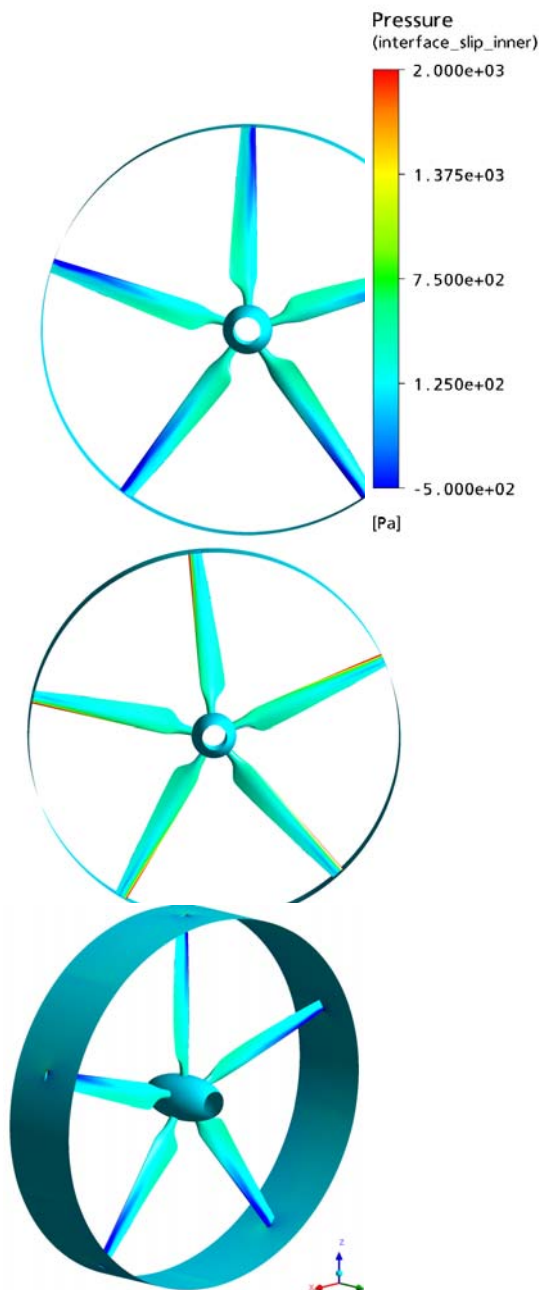


Figure 12: Pressure Distribution (gauge) on the pressure side (top), suction side (middle) and shroud of the rotor (bottom)

torque of the benchmark case was not recovered. We may conclude that the reason for the stable unsteady solution is the presence of the WDS increasing the air speed, as can be seen in Fig. 14, and thus modifying the relative angle, and Reynolds number allowing the flow to stabilize.

The following table summarizes the results obtained.

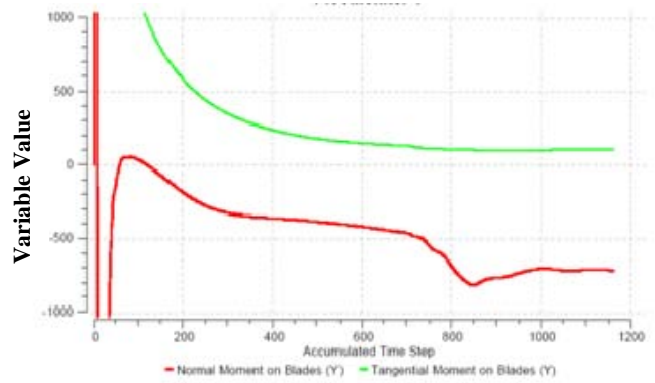


Figure 13: Convergence of the Normal and Tangential Moments. Red is normal moment and green is tangential moment.

Wind Speed Analysis	Tangential (N.m)	Normal(N.m)	Resultant torque(N.m)
7.0 m/s Steady	100	-700	-600
4.6 m/s Steady	-	-	-
4.6 m/s Unsteady	90	-560	-470

SUMMARY AND CONCLUSIONS

In this paper, a concept for using small wind turbines under conditions of low speed wind has been analyzed. This concept makes use of small turbines in clusters and uses a Wind Deflection Structure to amplify the wind speed. It was shown using both simple analysis and steady and unsteady CFD that the concept has merit. Using a cylinder in cross-flow analysis the relationship between the amplification factor vs. diameter ratio was quantified. The gain appears as a shift in the power-wind speed relationship to lower ambient air speeds. It was also

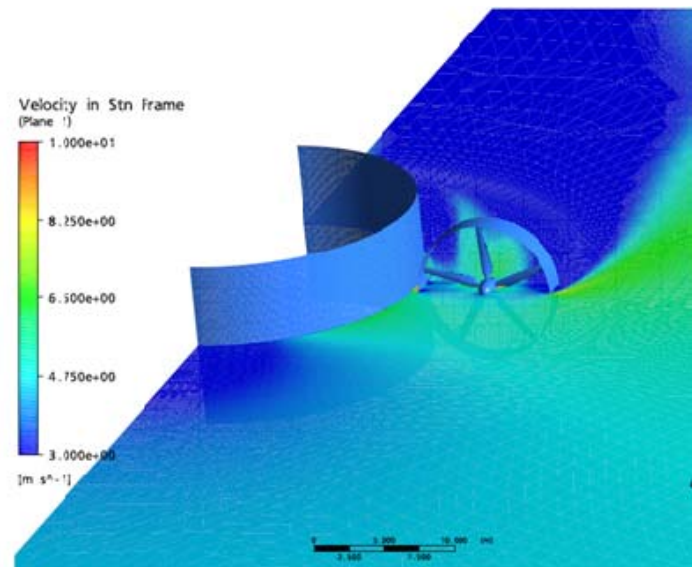


Figure 14: Velocity contours about the wind turbine

shown, using a standard test blade with a fixed pitch and constant RPM, that under low speeds, power may be derived with the use of a Wind Deflection Structure while without the WDS this may not be possible. The outcome was attributed to the ability of the WDS to raise the air speed to levels for which the blades can generate power. The power obtained using the WDS was 78% of the expected value for the case attempted thus suggesting that the amplification of graph of Fig. 4 and the resulting gain in power may be somewhat optimistic. Future work would include further analysis of the unsteady flow and studying placement of the rotor for optimum output.

ACKNOWLEDGEMENTS

This work was supported by a grant from the US Department of Energy (DOE). Guidance was provided by the National Renewable Energy Laboratory (NREL). The computational work was performed at NASA Glenn Research Center through a Space Act Agreement between NASA Glenn and The Ohio State University.

REFERENCES

- [1] American Wind Energy Association, June 2010, "Wind of Change," http://www.bluegreenalliance.org/press_room/publications?id=0048
- [2] Weisbrich, A. L. and Pucher, K., "Computational Fluid Dynamics Assessment of A WARP Wind Power System, Wind Power 1996, Denver, Colorado.
- [3] Krishnamurty Karamcheti, Principles of Ideal-Fluid Aerodynamics, Robert E. Krieger Publishing Company, 1966.
- [4] David A. Spera, Wind Turbine Technology, ASME Press, 1994.
- [5] Hand, M. M., Simms, D. A., Fingersh, L. J., Jager, D. W., Cotrell, J. R., Schreck, S. J., and Larwood, S. M., "Unsteady aerodynamics experiment phase VI: wind tunnel test configurations and available data campaigns," NREL/TP-500-29955, December 2001.
- [6] Potsdam, Mark and Mavriplis, Dimitri J. , "Unstructured Mesh CFD Aerodynamics Analysis of the NREL Phase VI Rotor," AIAA 2009- 1221, 47th AIAA Aerospace Sciences Meeting Including The New Horizons Forum and Aerospace Exposition.
- [7] Wilcox, D.C. (1988), "Reassessment of the scale-determining equation for advanced turbulence models", *AIAA Journal*, vol. 26, pp. 1414-1421.